

A study of quasi-elastic neutrino interactions in the NOMAD experiment



V. Lyubushkin^{1,2} **D. Naumov**¹ and **B. Popov**¹

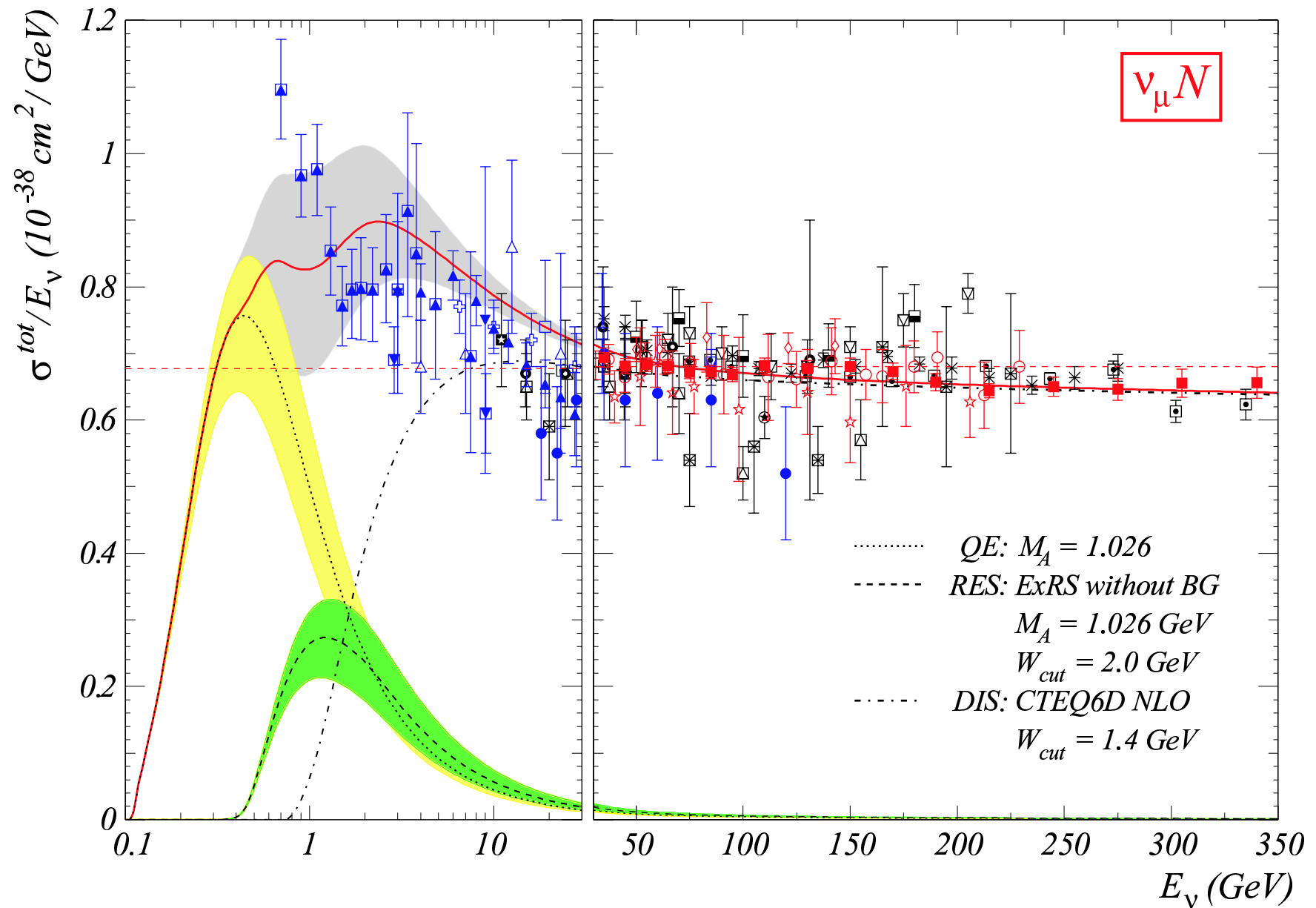
for the NOMAD Collaboration

¹ *Joint Institute for Nuclear Research, LNP, Dubna*

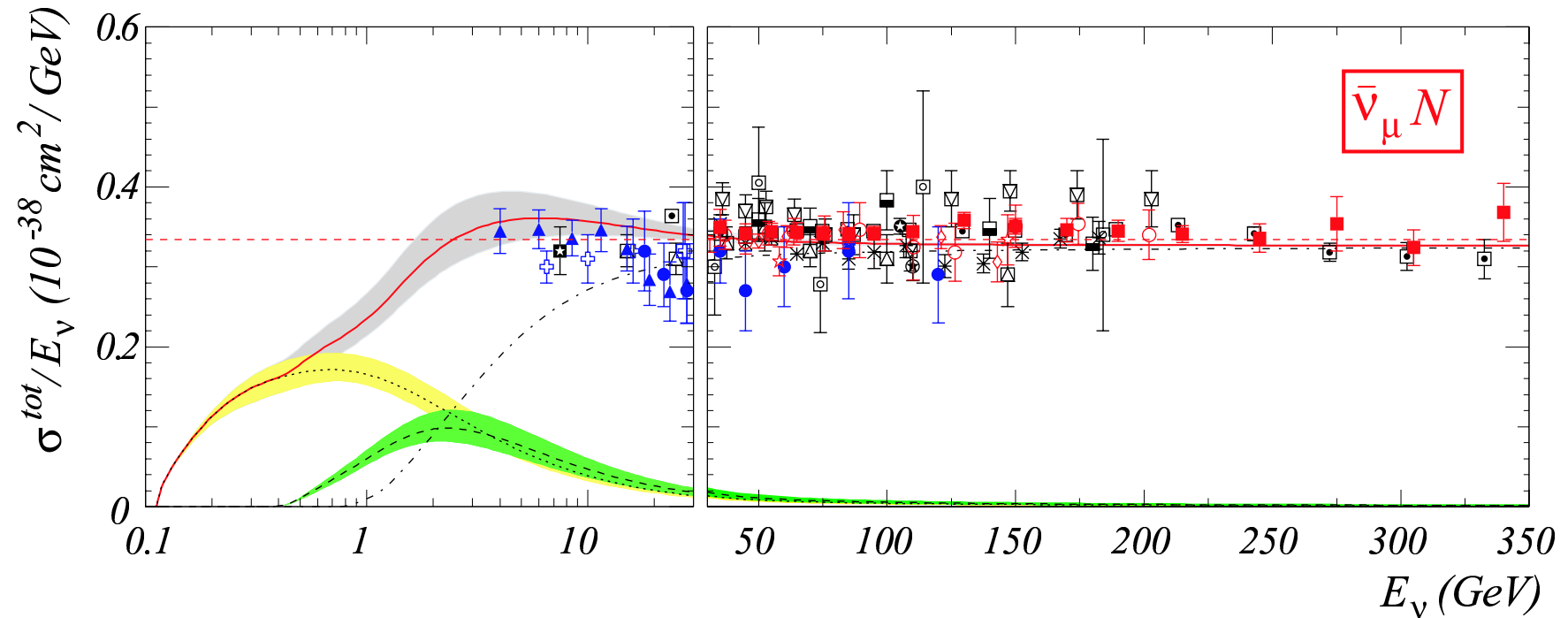
² *Physics Department of Irkutsk State University, Irkutsk*

- Phenomenology of $\nu_{\mu} + n \rightarrow \mu^{-} + p$ process
- Review of existing experimental data
- Description of the NOMAD detector
- Selection of quasi-elastic events (QEL)
- The QEL cross section measurement
- Our **results** and **conclusions**

The current status of the total ν_μ CC cross section



The current status of the total $\bar{\nu}_\mu$ CC cross section



▼ <i>Baltay et al., BNL 1980</i>	■ <i>Seligman, CCFR 1997</i>	⊙ <i>Shotton et al., CDHS 1985</i>
▲ <i>Baker et al., BNL 1982</i>	◻ <i>Naples, NuTeV 2003</i>	◊ <i>Berge et al., CDHS 1987</i>
◻ <i>Barish et al., CCFRR 1981</i>	◻ <i>Colley et al., BEBC 1979</i>	▼ <i>Allaby et al., CHARM 1988</i>
○ <i>MacFarlane et al., CCFRR 1984</i>	■ <i>Bosetti et al., BEBC 1982</i>	⊙ <i>Jonker et al., CHARM 1981</i>
★ <i>Auchincloss et al., CCFR 1990</i>	◻ <i>Allasia et al., BEBC 1984</i>	⊠ <i>Asratyan et al., IHEP-ITEP 1978</i>
● <i>Kitagaki et al., FNAL 1982</i>	▼ <i>Ciampolillo et al., GGM 1979</i>	△ <i>Baranov et al., IHEP SKAT 1979</i>
◻ <i>Taylor et al., HBF 1983</i>	● <i>Morfin et al., GGM 1981</i>	⊕ <i>Vovenko et al., IHEP-ITEP 1979</i>
⊠ <i>Baker et al., FNAL 1983</i>	* <i>Abramowicz et al., CDHS 1983</i>	▲ <i>Anikeev et al., IHEP-JINR 1996</i>

Phenomenology of $\nu_\mu n \rightarrow \mu^- p$ process

The most general form of the electroweak $N_{in} \rightarrow N_{out}$ transition current is given by ^a

$$J_\alpha = \langle N_{out}; p' | \hat{J}_\alpha | N_{in}; p \rangle = \bar{u}_p(p') \Gamma_\alpha u_n(p) \quad (1)$$

Here p and p' are the 4-momenta of the target nucleon N_{in} and final baryon N_{out} respectively. The the vertex 4-vector is

$$\Gamma_\alpha = \gamma_\alpha F_1 + i\sigma_{\alpha\beta} \frac{q^\beta}{2M} F_2 + \frac{q_\alpha}{M} F_S + \left(\gamma_\alpha F_A + \frac{p_\alpha + p'_\alpha}{M} F_T + \frac{q_\alpha}{M} F_P \right) \gamma_5 \quad (2)$$

The six form factors $F_i(Q^2)$ in the vertex function Γ_α are in general complex.

The most general restrictions to the form factors:

1. T invariance $\implies \text{Im}(F_V, F_M, F_A, F_P, F_S, F_T) = 0$;
2. C invariance $\implies \text{Im}(F_V, F_M, F_A, F_P) = 0$ and $\text{Re}(F_S, F_T) = 0$;
3. no SCC $\implies F_S = F_T = 0$ ($\equiv T$ invariance + C invariance);
4. $\partial_\alpha V^\alpha = 0$ (CVC) $\implies F_S = 0$.

^aC. H. Llewellyn Smith, "Neutrino reactions at accelerator energies," Phys. Rept. **3 C** (1972) 261–379.

Electromagnetic form factors

We have investigated several models for the nucleon electromagnetic Sachs form factors

$$G_E(Q^2) = F_1(Q^2) - \frac{Q^2}{4M_i^2} F_2(Q^2) \quad \text{and} \quad G_M(Q^2) = F_1(Q^2) + F_2(Q^2)$$

where $F_1(Q^2)$ and $F_2(Q^2)$ are the Dirac and Pauli form factors, respectively.

- ❖ Simple dipole parametrization:

$$G_E(Q^2) = G_M(Q^2) / (\mu_p - \mu_n) = G_D(Q^2) = (1 + Q^2/0.71)^{-2}$$

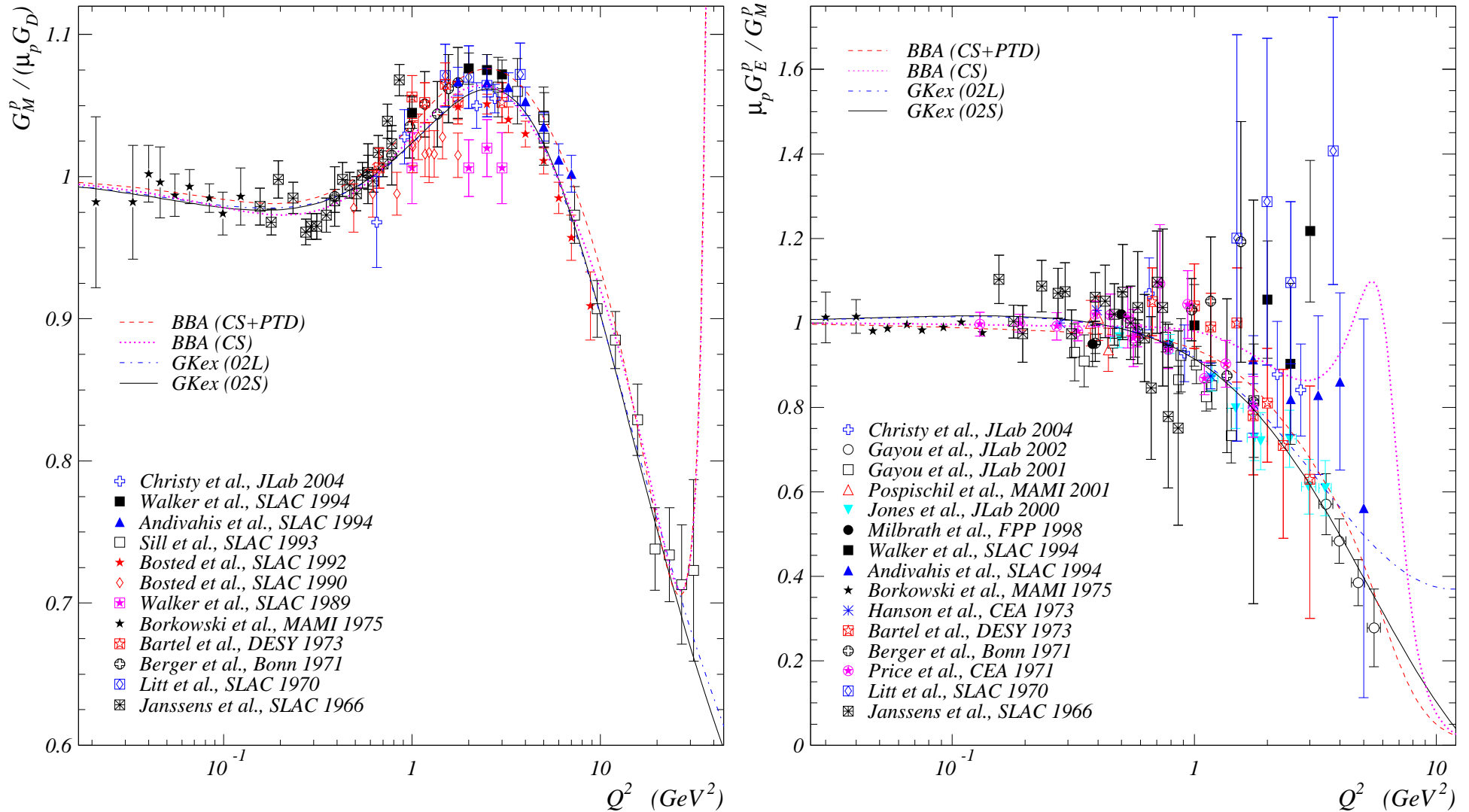
- ❖ Gari–Krümpelmann (GK) model^a extended and fine-tuned by Lomon^b to match current experimental data. Specifically, as the “reference model”, we explore the so-called GKex(02S) which fits the modern and consistent older data well and meets the requirements of dispersion relations and of QCD at low and high 4-momentum transfer.
- ❖ Global fit by Budd *et al.*,^c (BBA model) to the data from Rosenbluth analysis of elastic ep cross section measurements and those from the polarization transfer techniques.

^aM. F. Gari and W. Krümpelmann, “The electric neutron form factor and the strange quark content of the nucleon,” Phys. Lett. B **274** (1992) 159-162; erratum – *ibid.* **282** (1992) 483-484.

^bE. L. Lomon, “Effect of recent R_p and R_n measurements on extended Gari–Krümpelmann model fits to nucleon electromagnetic form factors,” Phys. Rev. C **66** (2002) 045501 [nucl-th/0203081].

^cH. Budd, A. Bodek, and J. Arrington, “Modeling quasi-elastic form factors for electron and neutrino scattering,” hep-ex/0308005, to be published in Nucl. Phys. B (Proc. Suppl.).

Proton electromagnetic form factors

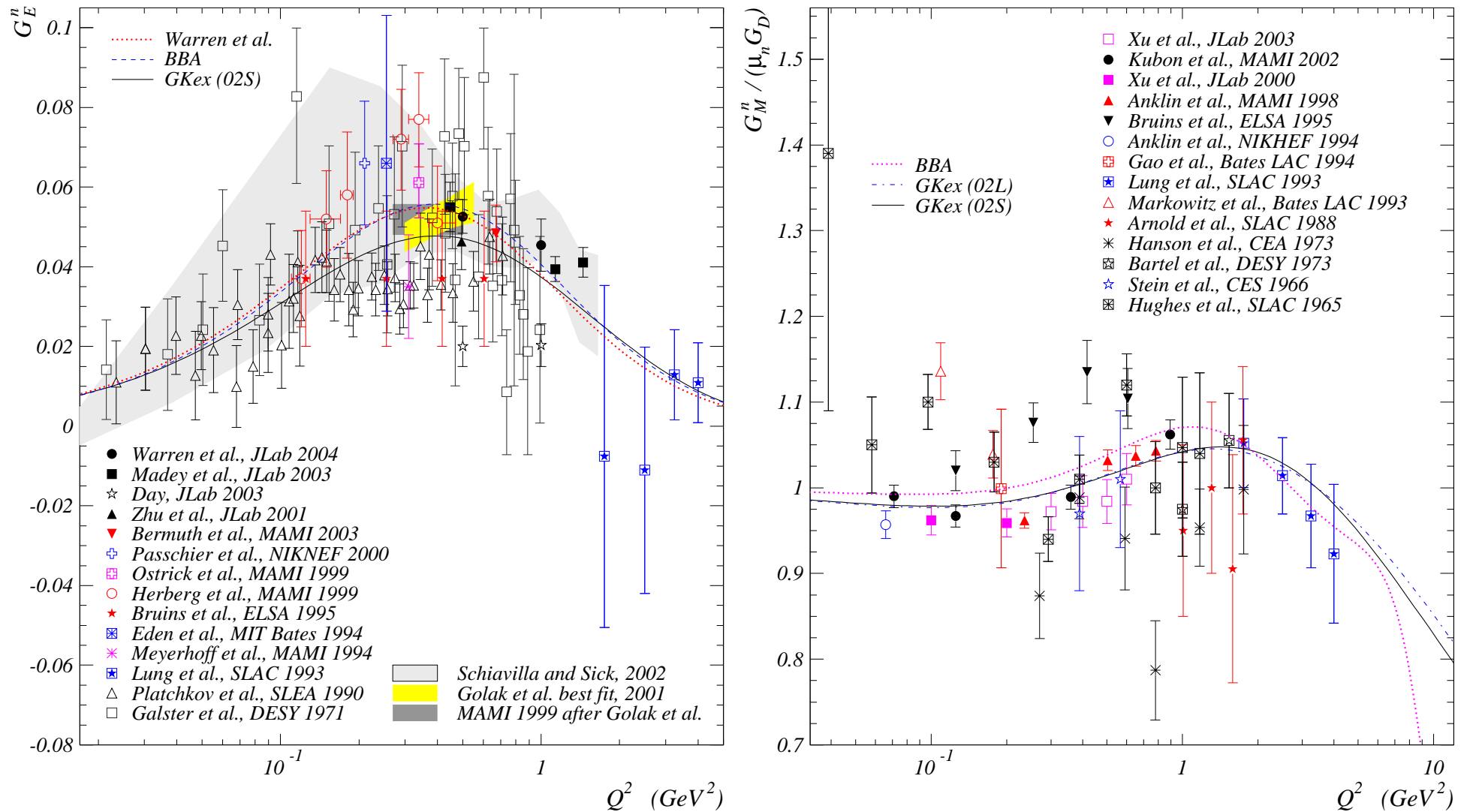


Normalized magnetic form factor and ratio of electric and magnetic form factors of the proton.

BBA: Budd-Bodek-Arrington [hep-ex/0308005] global fit to the data from Rosenbluth analysis of elastic ep cross section measurements and those from the polarization transfer techniques.

GKex: extended Gari-Krümpelmann model after Lomon [PRC **66** (2002) 045501].

Neutron electromagnetic form factors



Electric and normalized magnetic form factors of the neutron. Together with the **BBA** and **GKex** fits (see previous slide), the recent fit by Warren *et al.* [PRL **92** (2004) 042301] is also shown. The filled areas represent some theoretical extractions from different data subsets.

Axial and pseudoscalar form factors

The customary parametrizations for the axial and pseudoscalar form factors are

$$F_A(q^2) = F_A(0) \left(1 - \frac{q^2}{M_A^2}\right)^{-n} \quad \text{with} \quad n = \begin{cases} 2 & \text{("dipole")}, \\ 1 & \text{("monopole")}; \end{cases}$$

$$F_P(q^2) = \frac{2M^2}{m_\pi^2 - q^2} F_A(q^2) \quad (\text{PCAC}) \quad \text{and} \quad F_A(0) = g_A = -1.2695 \pm 0.0029.$$

The pseudoscalar contribution is important for τ production.^a Note that the "standard" expression for the F_P is at most a (doubtful) parametrization inspired by the PCAC hypothesis (+ pion pole dominance near $q^2 = 0$).

The experiments on QE and pion electroproduction permit very wide spread of M_A :

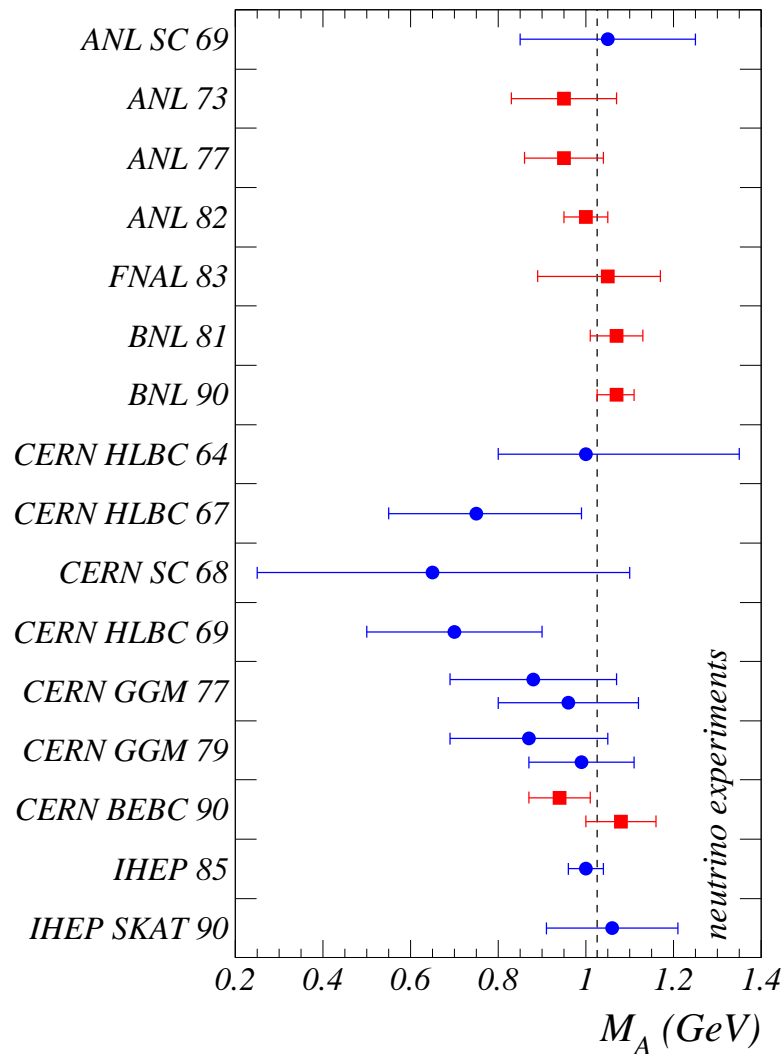
from roughly 0.7 to 1.2 GeV/ c^2 for dipole F_A ,

from roughly 0.6 to 0.8 GeV/ c^2 for monopole F_A .

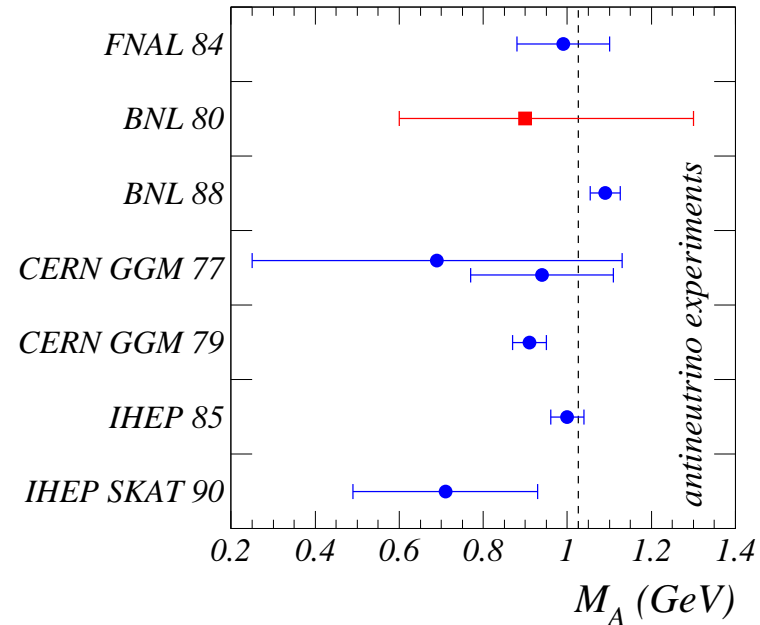
However the monopole parametrization seems to be obsolete.

^aK. Hagiwara, K. Mawatari and H. Yokoya, "Pseudoscalar form factors in tau-neutrino nucleon scattering," hep-ph/0403076; see also poster by H. Yokoya in this workshop.

Axial form factor from neutrino scattering experiments



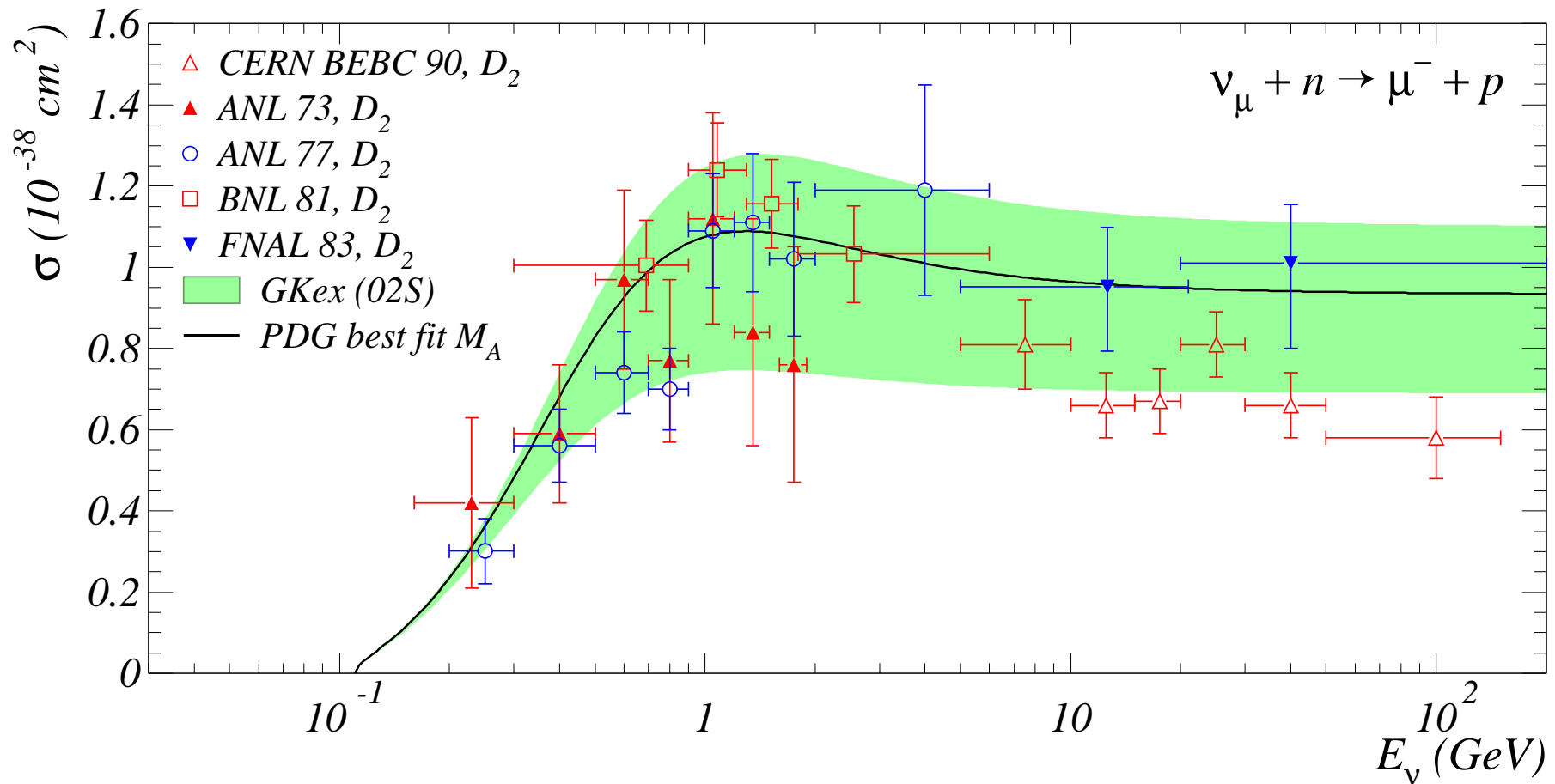
- Deuterium filled bubble chambers
- Heavy liquid bubble chambers and spark chambers
- ⋮ M_A world average value



Axial mass average value $M_A = 1.026 \pm 0.021$ GeV was borrowed from review by V. Bernard *et al.*^a

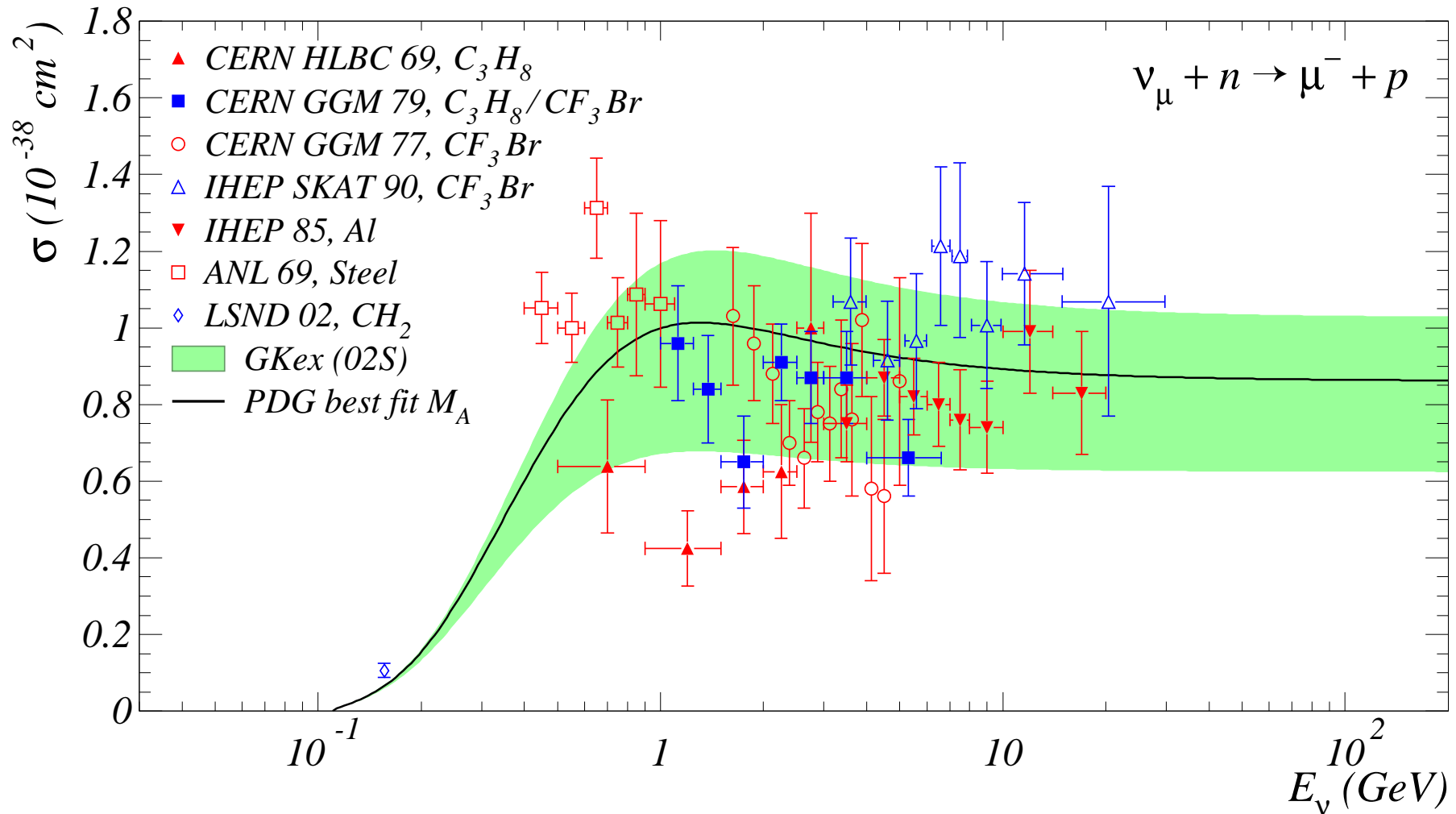
^aV. Bernard, L. Elouadrhiri and Ulf-G. Meißner, "Axial structure of the nucleon," J. Phys. G **28** (2002) R1–R35 [hep-ph/0107088].

Total QE $\nu_\mu n$ cross section from deuterium filled bubble chambers



Total QE $\nu_\mu n$ cross section extracted from $\nu_\mu D$ scattering data. All the data are corrected to nuclear effects. The theoretical band corresponds to variations of M_A from 0.7 to 1.2 GeV.

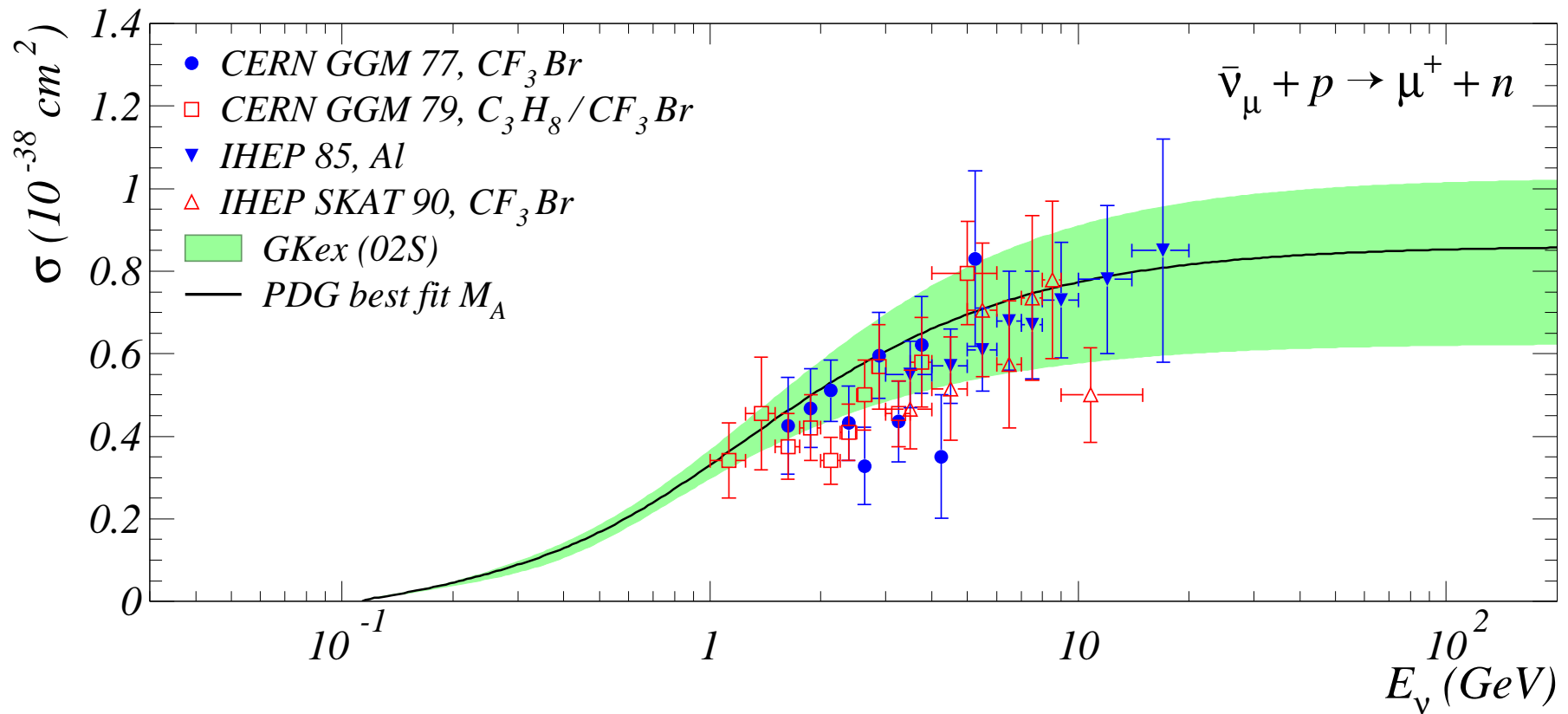
Total QE $\nu_\mu n$ cross section measured on heavy nuclei target



Total QE cross $\nu_\mu n$ cross section extracted from the data on ν_μ scattering off heavy nuclei. Nuclear effects are included into calculations according to the standard relativistic Fermi gas model.^a The theoretical band corresponds to variations of M_A from 0.7 to 1.2 GeV/ c^2 .

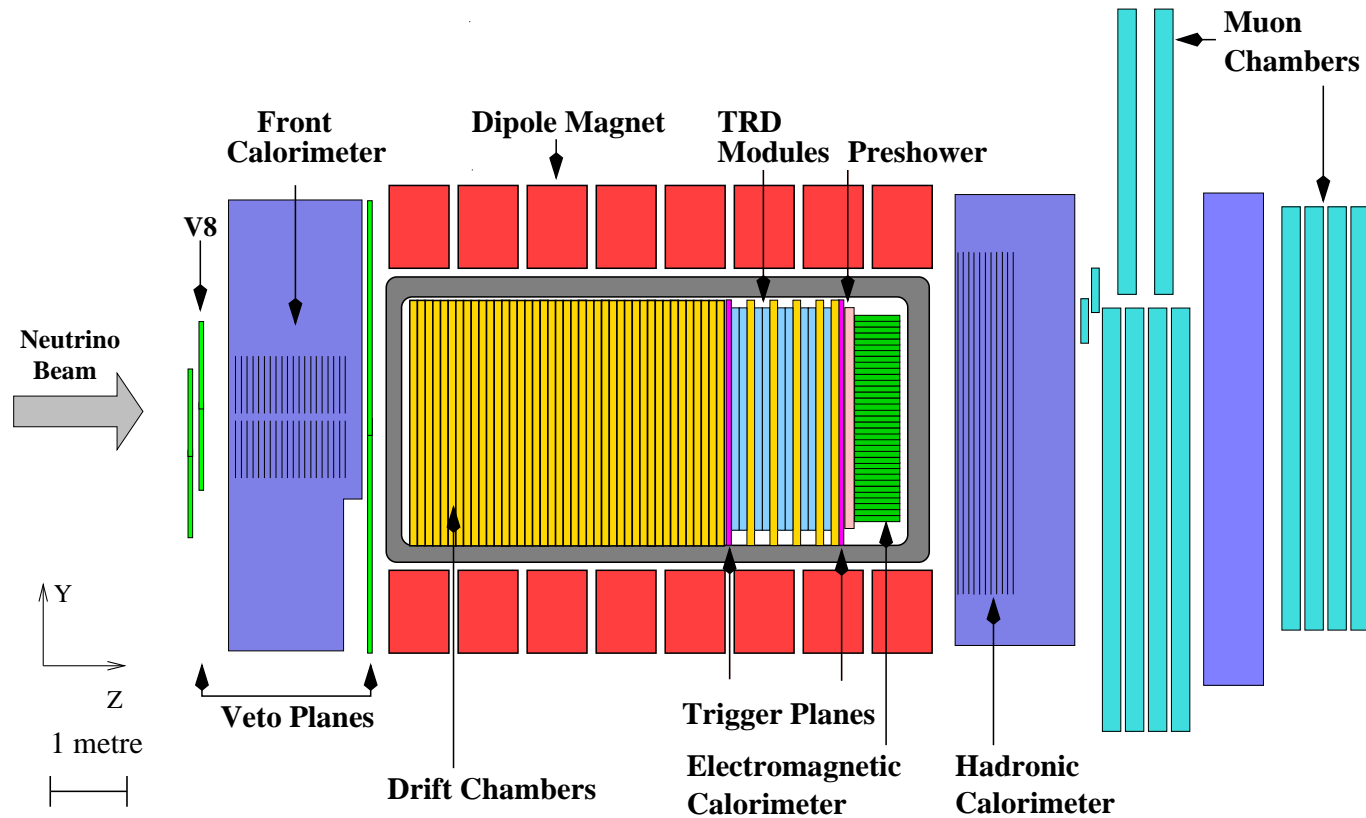
^aR. A. Smith and E. J. Moniz, "Neutrino reactions on nuclear targets," Nucl. Phys. B **43** (1972) 605–622; erratum – *ibid.* **101** (1975) 547.

Total QE cross $\bar{\nu}_\mu p$ cross section measured on heavy nuclei target



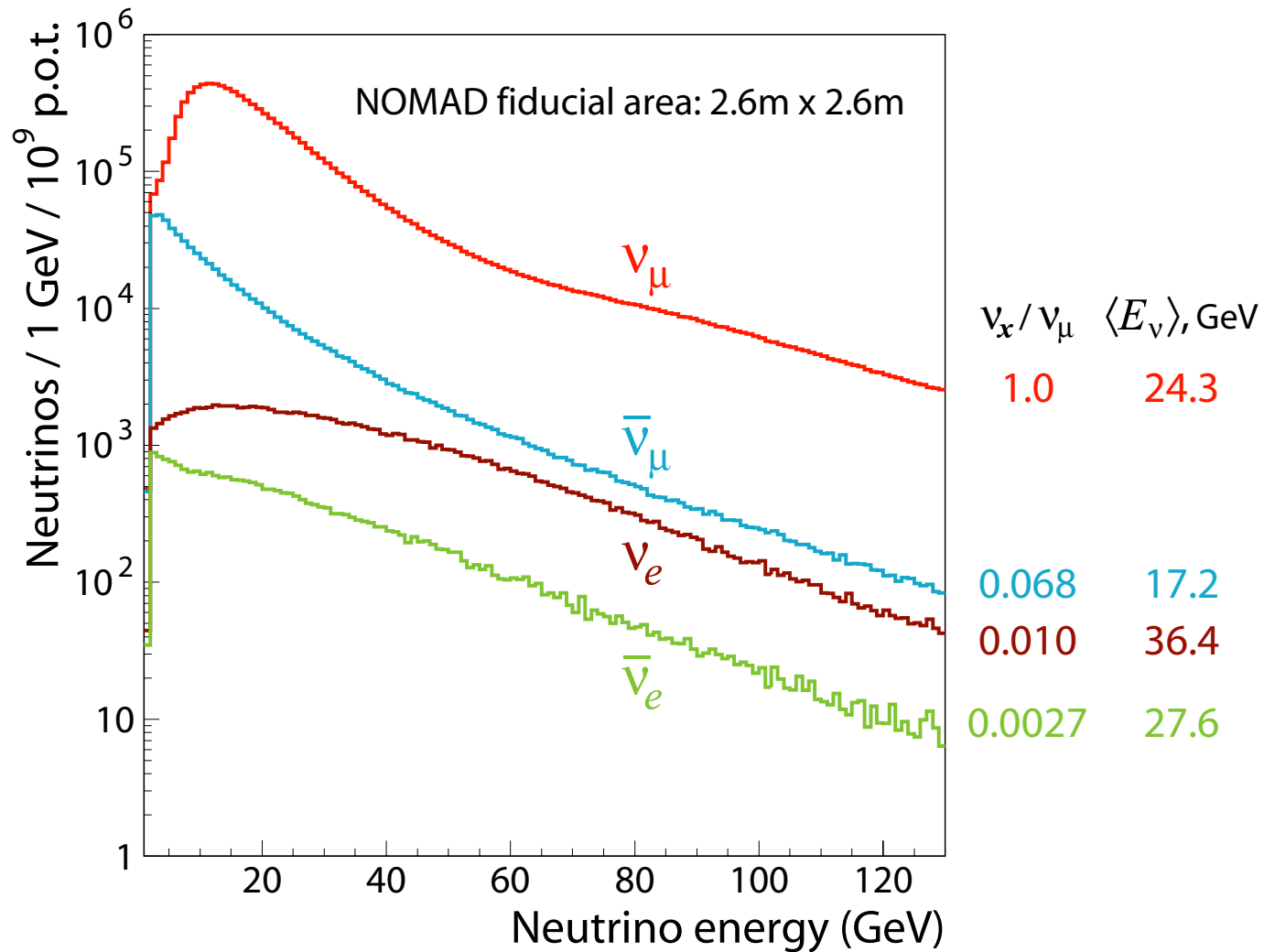
Total QE cross $\bar{\nu}_\mu p$ cross section extracted from the data on $\bar{\nu}_\mu$ scattering off heavy nuclei. Nuclear effects are included into calculations according to the relativistic Fermi gas model by Smith and Moniz (see previous slide for the reference). The theoretical band corresponds to variations of M_A from 0.7 to 1.2 GeV/c^2 .

NOMAD experiment



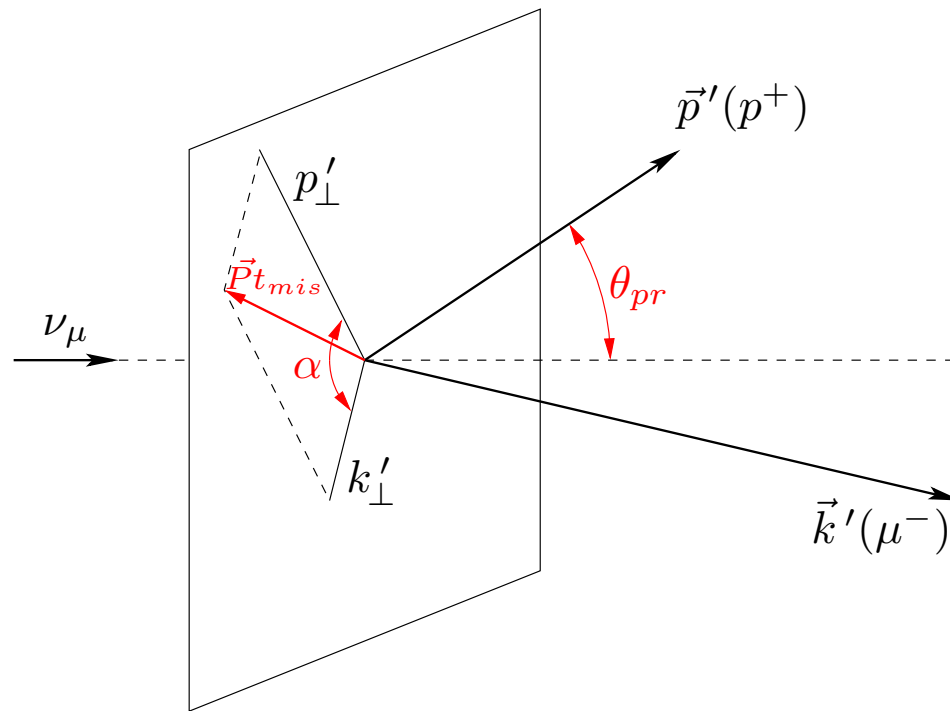
- **Drift Chambers** (target and momentum measurement) Position resolution $< 200 \mu\text{m}$ (small angle tracks)
Momentum resolution $\sim 3.5\%$ ($p < 10 \text{ GeV}/c$)
- **Transition Radiation Detector** for e^\pm identification: π rejection $\sim 10^3$ for electron efficiency $\geq 90\%$
- Lead glass **Electromagnetic Calorimeter** $\frac{\sigma(E)}{E} = (1.04 \pm 0.01)\% + \frac{(3.22 \pm 0.07)\%}{\sqrt{E(\text{GeV})}}$
- **Muon Chambers** for μ^\pm identification: efficiency $\approx 97\%$ ($p_\mu > 5 \text{ GeV}/c$)
- **Hadronic Calorimeter** for n and K_L^0 veto

Neutrino fluxes at NOMAD experiment



P. Astier *et al.* [NOMAD Collaboration], "Prediction of neutrino fluxes in the NOMAD experiment," Nucl. Instrum. Meth. A **515**, 800 (2003) [arXiv:hep-ex/0306022].

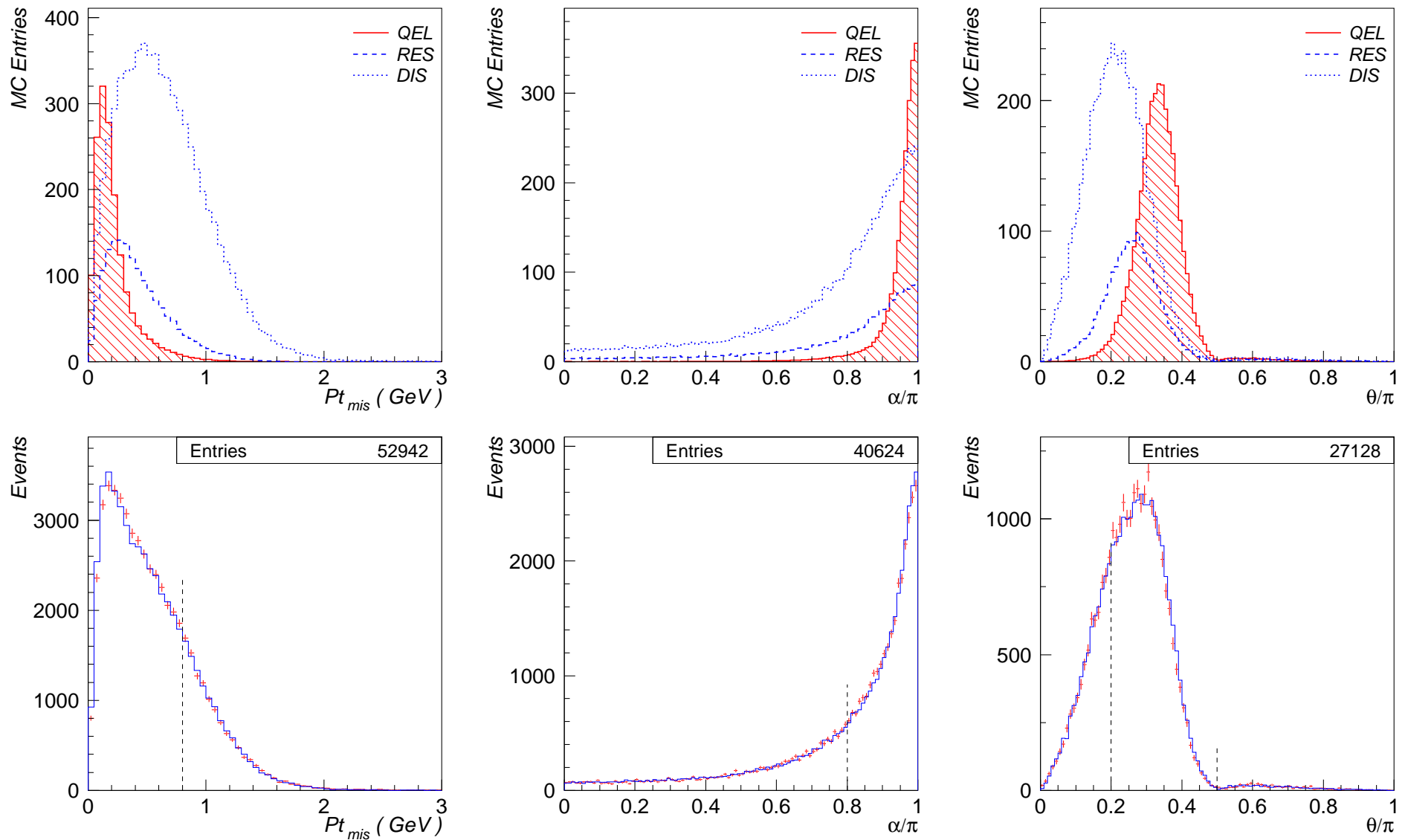
Reconstructed kinematical variables



- $E_\nu = k'_z + p'_z$
- $E_\ell = \left(|\vec{k}'|^2 + m_\ell^2\right)^{1/2}$
- $Q^2 = 2E_\nu(E_\ell - k'_z) - m_\ell^2$
- $W^2 = m_i^2 + 2m_i(E_\nu - E_\ell) - Q^2$

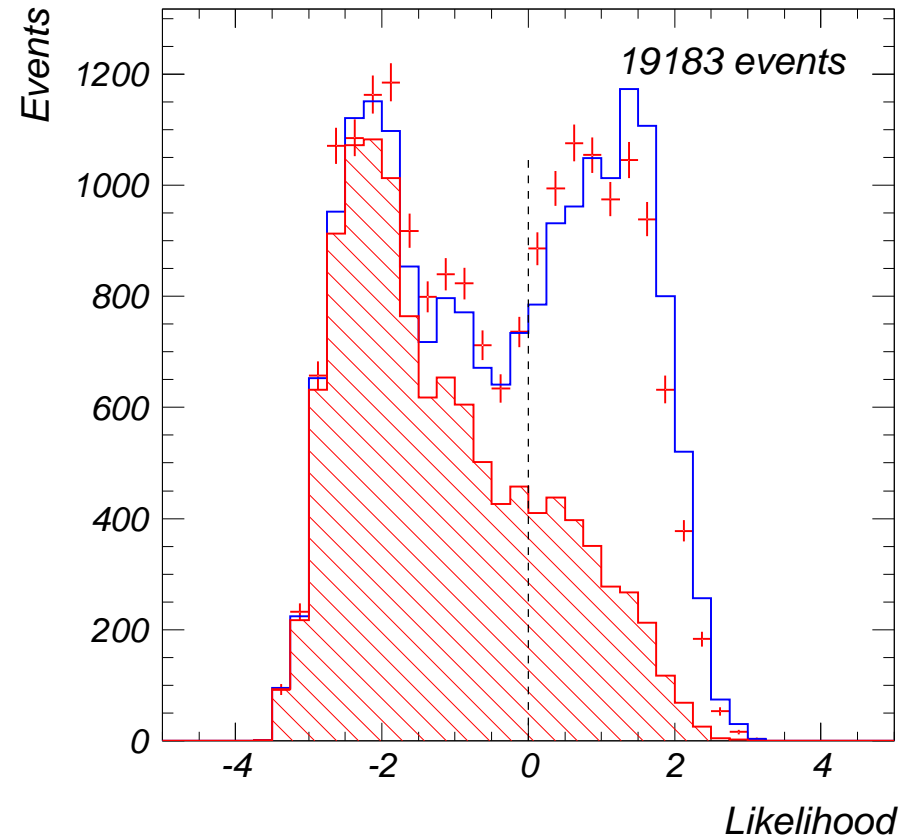
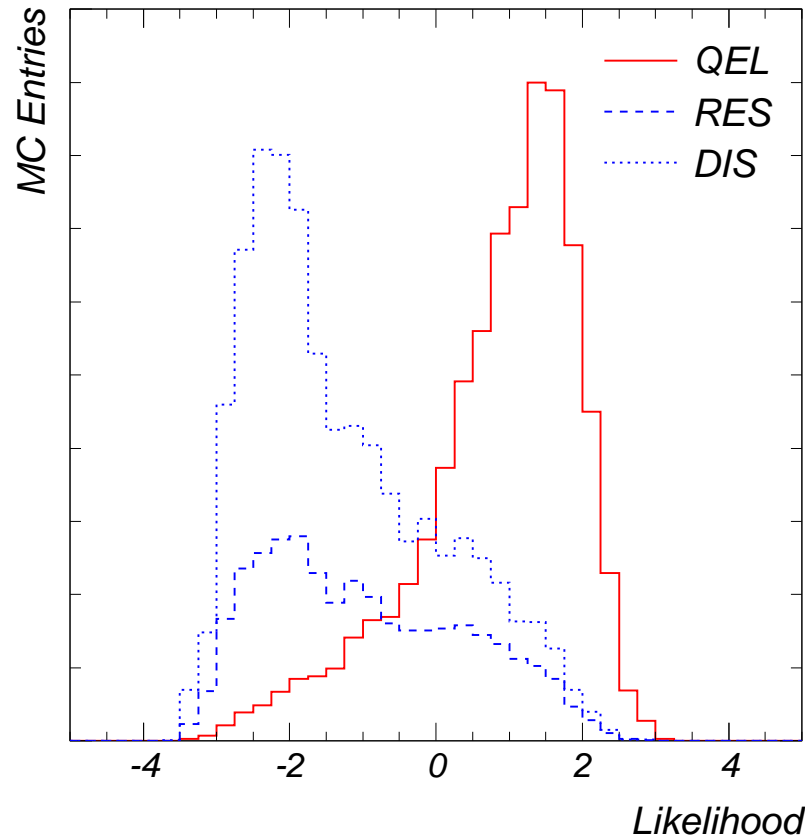
- ✓ reconstructed primary vertex should be in the selected fiducial volume:
 $|X, Y| \leq 120 \text{ cm}, 5 \leq Z \leq 395 \text{ cm}$
- ✓ only two charged tracks from the primary vertex (here we do not take into account neutral tracks): one of them should be identified as the muon track while the second track should correspond to a positively charged particle
- ✓ number of hits associated with the positively charged track should be greater than 7
- ✓ reconstructed neutrino energy $1 \leq E_\nu \leq 100 \text{ GeV}$
- ✓ reconstructed invariant hadronic mass $0 \leq W^2 \leq 1.76 \text{ GeV}^2$

Likelihood variables in simulated events and experimental data



Missing transverse momentum Pt_{mis} , angle α between the transverse components of the charged primary tracks and angle θ_{pr} between the proton momentum and z axis. Distributions for simulated events of different modes (top). Comparison of expected and experimental data distributions (bottom).

Likelihood ratio



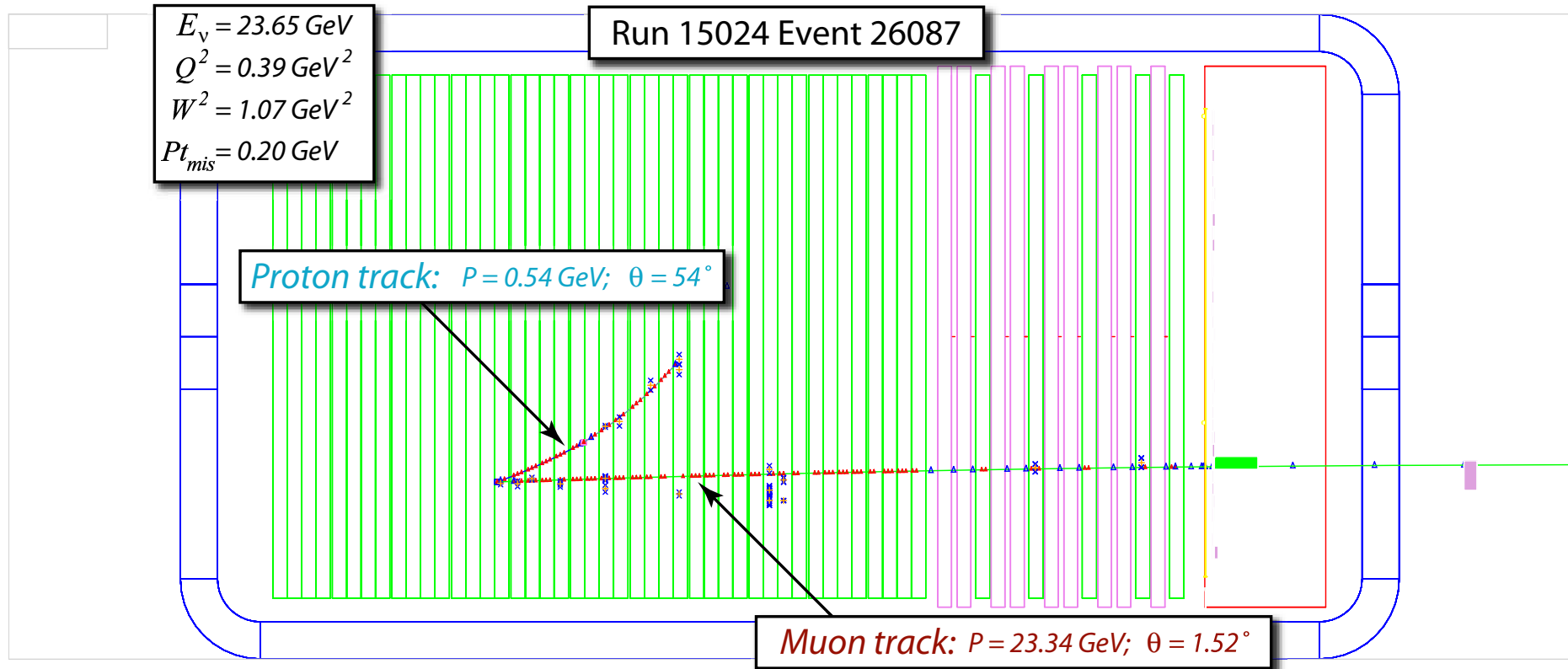
The set of variables $\vec{\ell} = \{Pt_{mis}, \theta_{pr}, \alpha\}$ can be associated with some likelihood ratio:

$$\mathcal{L} = \ln \frac{P(\vec{\ell} | QEL)}{P(\vec{\ell} | RES)}$$

where $P(\vec{\ell} | QEL)$ and $P(\vec{\ell} | RES)$ are the probabilities for the signal and background events to have kinematic variables $\vec{\ell}$.

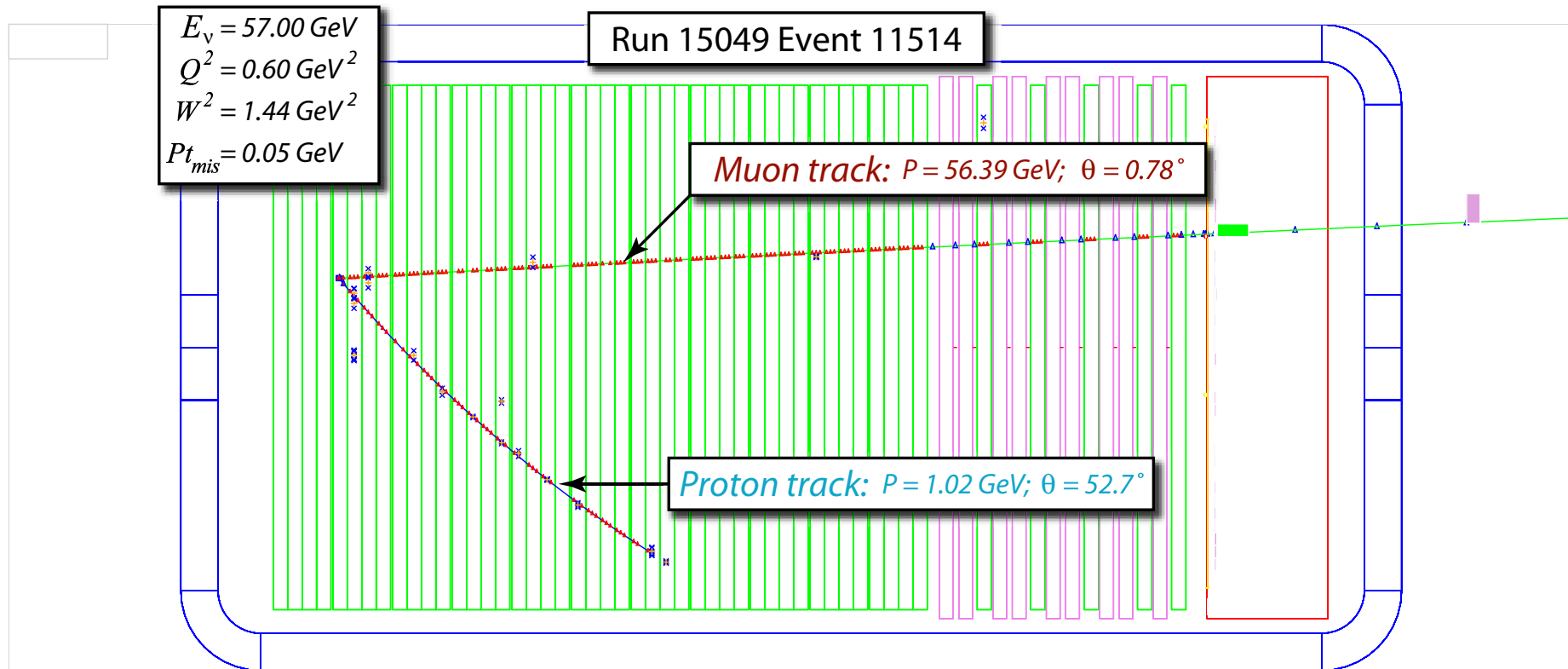
8235 events were found. Expected **purity** of quasi-elastic events in the final sample is **70.5%** and the total **efficiency** is **23.8%**.

View of typical QEL candidate event in NOMAD detector



Typical examples of data events identified as $\nu_\mu + n \rightarrow \mu^- + p$ (run 15024 event 26087). Long track is identified as negatively charged muon, short track is associated with proton.

View of typical QEL candidate event in NOMAD detector



Typical examples of data events identified as $\nu_\mu + n \rightarrow \mu^- + p$ (run 15049 event 11514). Long track is identified as negatively charged muon, short track is associated with proton.

QEL cross section measurement: normalization to Deep Inelastic Scattering

- ✓ the primary vertex should be in the chosen fiducial volume:
 $|X, Y| \leq 120 \text{ cm}, 5 \leq Z \leq 395 \text{ cm}$
- ✓ at least two charged tracks at the primary vertex, one of them should be identified as a muon
- ✓ (1) the total visible energy in the event $1 \leq E_\nu \leq 300 \text{ GeV}$ and the reconstructed hadronic mass squared $W \geq 1.4 \text{ GeV}$

$$\langle \sigma_0 \rangle = \langle \sigma_{dis} \rangle^a = 15.608 \cdot 10^{-38} \text{ cm}^2, \quad N_0 = 1260542$$

- ✓ (2) the total visible energy in the event $40 \leq E_\nu \leq 200 \text{ GeV}$ and the reconstructed hadronic mass squared $W \geq 1.4 \text{ GeV}$

$$\langle \sigma_0 \rangle = \langle \sigma_{dis} \rangle^a = 6.101 \cdot 10^{-38} \text{ cm}^2, \quad N_0 = 465954$$

- ✓ (3) the total visible energy in the event $40 \leq E_\nu \leq 200 \text{ GeV}$

$$\langle \sigma_0 \rangle = \langle \sigma_{dis} \rangle^b = 6.317 \cdot 10^{-38} \text{ cm}^2, \quad N_0 = 478657$$

^a A. Bodek and U. K. Yang, "Modeling deep inelastic cross sections in the few GeV region," Nucl. Phys. B (Proc. Suppl.) **112** (2002) 70–76 [arXiv:hep-ex/0203009]; A. Bodek and U. K. Yang, "Higher twist, ξ_w scaling, and effective LO PDFs for lepton scattering in the few GeV region," J. Phys. G **29** (2003) 1899–1906 [arXiv:hep-ex/0210024].

^b We assume $\sigma_{dis}(E_\nu)/E_\nu = 0.677 \times 10^{-38} \text{ cm}^2$; S. Eidelman *et al.* (Particle Data Group), Phys. Lett. B **592** (2004) 1–1109

Systematic uncertainties

- ✓ QEL Identification procedure. We can estimate this uncertainty by varying the selection criteria within reasonable limits.
- ✓ Uncertainty in the DIS cross-section, used for normalization. Uncertainty of the single pion production cross-section.
- ✓ Uncertainty induced from nuclear-structure effects. As was shown in paper ^a such kind of effects are important and should be taken into account carefully.
- ✓ Uncertainty in the proton detection efficiency due to nuclear effects.

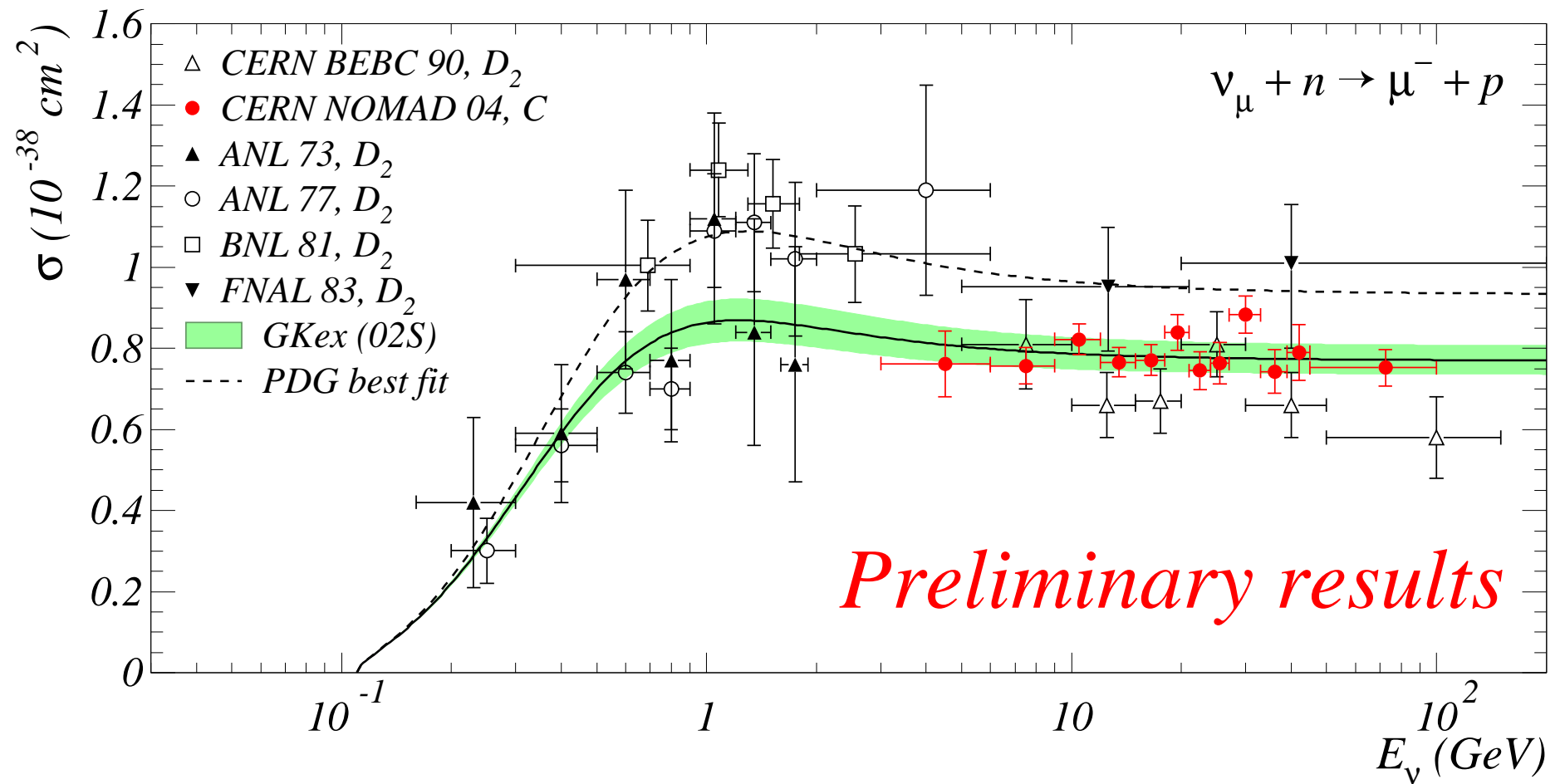
ESTIMATE OF SYSTEMATIC UNCERTAINTIES NOT YET COMPLETED

$$\delta(\langle\sigma_{qel}\rangle)_{syst} = 0.0? \times 10^{-38} \text{ cm}^2.$$

$$\sigma_{qel} = [0.72 \pm 0.01(stat) \pm 0.0?(syst)] \cdot 10^{-38} \text{ cm}^2$$

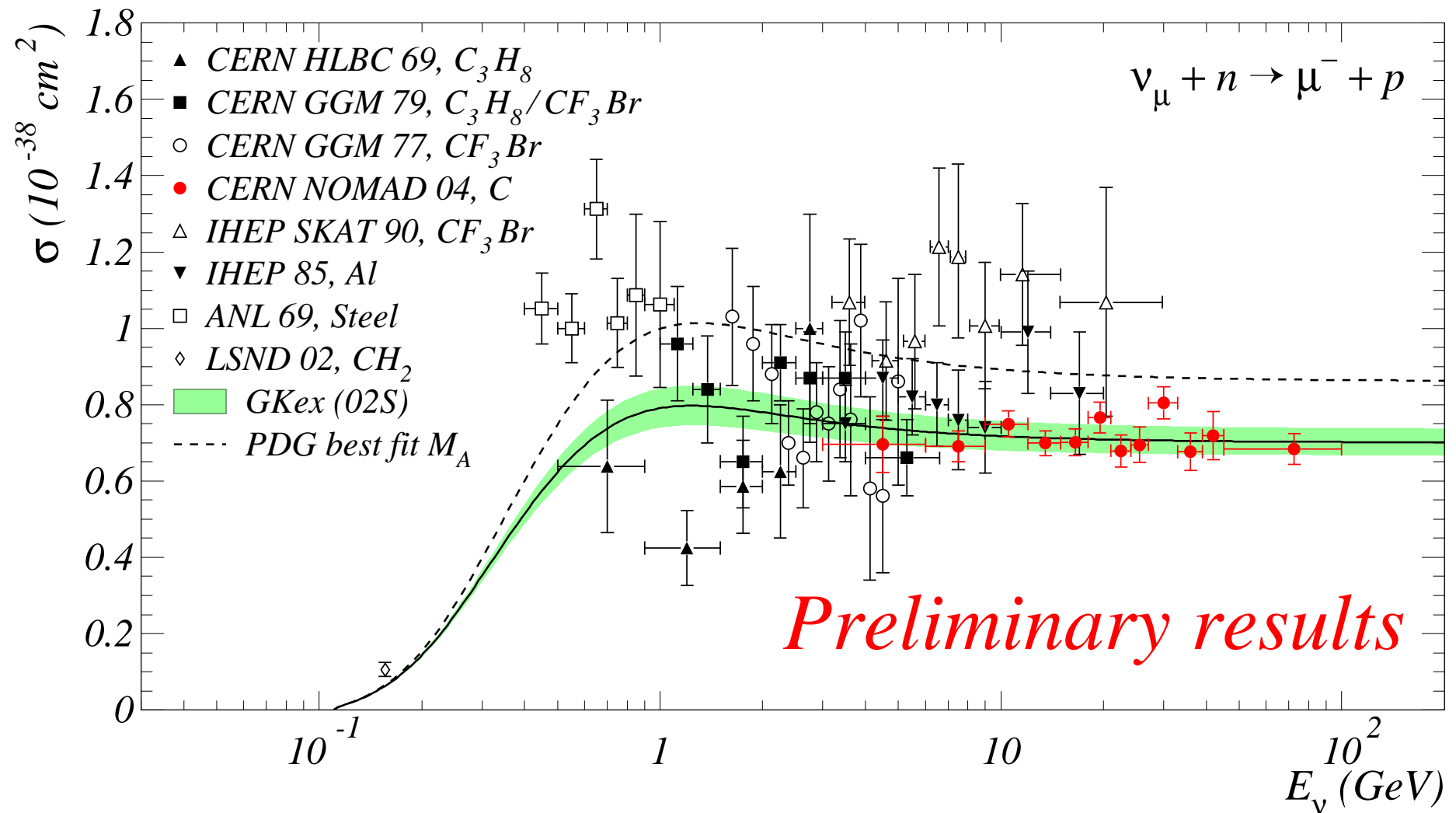
^aH. c. Kim, J. Piekarewicz and C. J. Horowitz, "Relativistic nuclear structure effects in quasielastic neutrino scattering," Phys. Rev. C **51**, 2739 (1995) [arXiv:nucl-th/9412017].

Comparison with previous experimental data



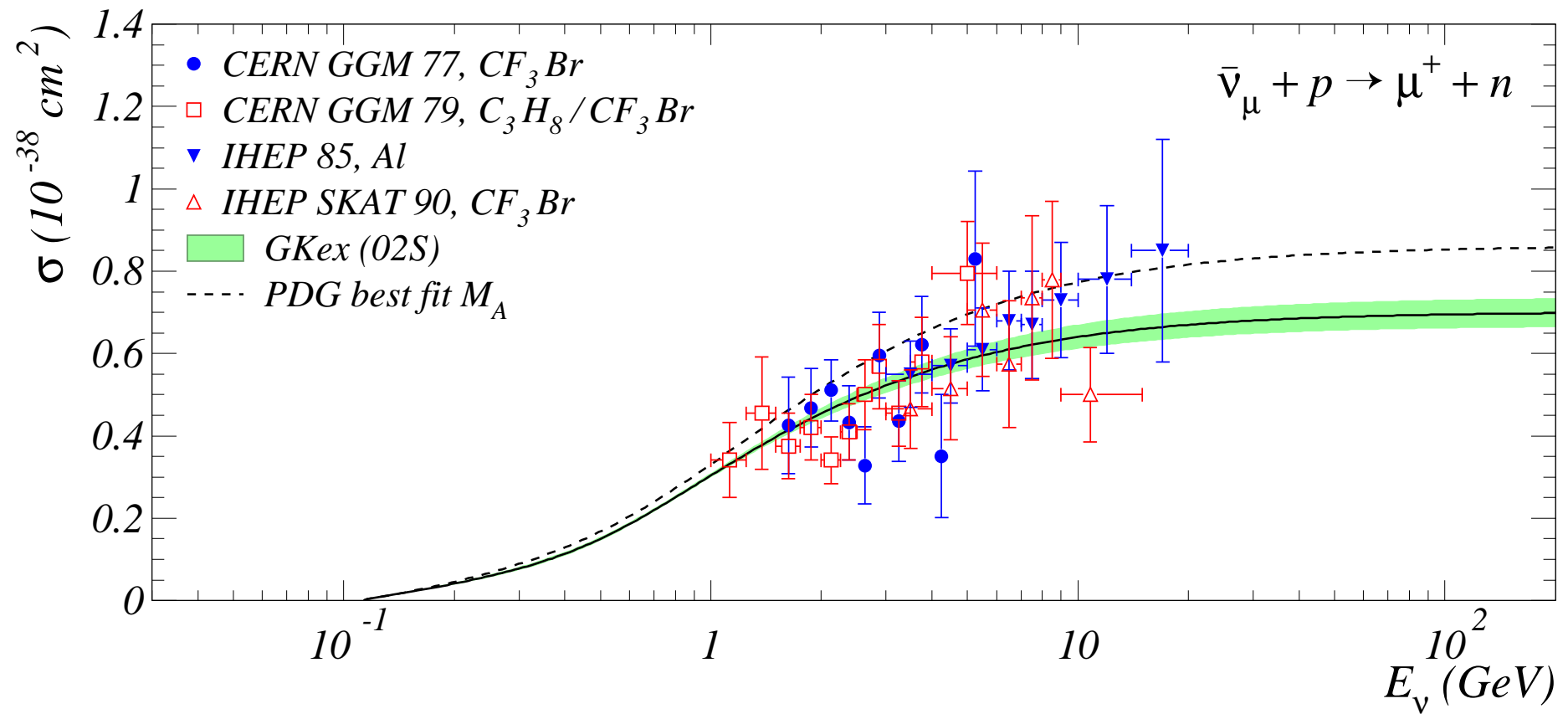
Comparison with previous experimental data from deuterium filled bubble chambers. All experimental data are corrected to nuclear effects.

Comparison with previous experimental data



Comparison with previous experimental data extracted from the data on ν_{μ} scattering off heavy nuclei. Nuclear effects are included into calculations according to the standard relativistic Fermi gas model. The theoretical band corresponds to both statistical and systematical uncertainties.

Comparison with previous experimental data



The total cross-section of $\bar{\nu}_\mu p \rightarrow \mu^+ n$ process extracted from the data on $\bar{\nu}_\mu$ scattering off heavy nuclei. Nuclear effects are included into calculations according to the standard relativistic Fermi gas model.

Conclusion

- ✓ We analyse 1.3×10^6 ν_μ *CC* events and identify 8235 QEL candidates with about 30% background contamination from the DIS and RES events. Total efficiency of QEL selection is about 24%.
- ✓ The $\nu_\mu + n \rightarrow \mu^- + p$ cross-section measurement is performed with normalization to deep inelastic scattering: ^a

$$\sigma_{qel} = [0.72 \pm 0.01(stat) \pm 0.0?(syst)] \cdot 10^{-38} \text{ cm}^2$$

- ✓ We performed the most up to date statistical accurate measurement of the $\nu_\mu + n \rightarrow \mu^- + p$ cross-section and corresponding axial mass of the dipole parametrization of the axial form-factor. The measured cross-section is about 20% below the current world average value.

^aHere we give $\langle \sigma_{qel} \rangle$ per 1 neutron in the light isoscalar nuclear target. We take into account only neutron content of the NOMAD target without converting $\langle \sigma_{qel} \rangle$ to free initial nucleon.